J. Phys. D: Appl. Phys., 1971, Vol. 4. Printed in Great Britain

Reflectivity and curvature of hypersonic shock waves at 1 atmosphere

D. SIMPSON† and P. R. SMY

Department of Electrical Engineering, University of Alberta, Edmonton, Alberta, Canada

MS. received 10*th November* 1970

Abstract. The reflectivity and curvature of a shock front moving into air at 1 atmosphere at velocities of up to Mach 10 are determined experimentally and the results compared with theory. It is found that whilst the reflectivity of the shock front is in good agreement with the expected values, the curvature is greater than that predicted at the highest Mach numbers.

1. Introduction

The technique of using measurements of the optical reflectivity of a shock front to determine the structure and thickness of the shock front was pioneered by Hornig and his co-workers (Cowan and Hornig 1950, Greene *et al.* 1951, Greene and Hornig 1953), but the use of the technique has been severely limited by a systematic departure (attributed to shock front curvature (Linzer and Hornig 1963)) of the experimental observations from the theory used. Shock curvatures have been measured by means of an array of pressure probes by Duff and Young (1961) and Mazzella and DeBoer (1966), but the range of Mach numbers and pressures involved has not been extensive. Simpson and Smy (1969) and Pert *et al.* (1970) have used optical reflection measurements to determine simultaneously the reflectivity and curvature of shock fronts moving at velocities of up to Mach 3 at various pressures, and have obtained good agreement with the exact theory of reflection of Pert and Smy (1970).

In this paper the optical reflectivity method is used to extend the measurements of reflection coefficient and curvature to hypersonic (Mach 10) velocities, at an ambient pressure of 1 atmosphere.

2. Theory

2.1. *Reflection of a light beam from a density discontinuity*

For a refractive index discontinuity, n to $n+\delta n$, classical electromagnetic theory may be used to derive the Fresnel formulae (Born and Wolf 1970)

$$R_{\parallel}=\left(\frac{\tan(\theta_0-\theta_1)}{\tan(\theta_0+\theta_1)}\right)^2 \tag{1}$$

$$R_{\perp}=\left(\frac{\sin(\theta_0-\theta_1)}{\sin(\theta_0+\theta_1)}\right)^2 \tag{2}$$

where $R_{\parallel}$ and $R_{\perp}$ are the intensity reflection coefficients for the components of the electric field vector parallel and perpendicular to the reflecting plane, respectively, and θ_0, θ_1 are the angles of incidence and refraction (transmission).

At grazing incidence, as used in all the experiments described or cited,

$$R_{\parallel}=R_{\perp}=R_1=\left(\frac{\theta_0-\theta_1}{\theta_0+\theta_1}\right)^2 \tag{3}$$

† Present address: Electricity Council Research Centre, Capenhurst, Chester, England.

which may be expanded in terms of the grazing angle of incidence, θ'_0 ($=\frac{1}{2}\pi-\theta_0$) and the refractive indices (n, $n+\delta n$) to give

$$R_1=\frac{1}{4\theta'_0{}^4}\left(\frac{\delta n}{n}\right)^2\left\{1-\frac{1}{\theta'_0{}^2}\left(\frac{\delta n}{n}\right)+\ldots\right\}. \tag{4}$$

In the case of a shock wave, however, there is a finite refractive index gradient at the shock front, which gives rise to three second-order effects, all of which tend to reduce the reflectivity R below the value R_1 (equation (4)) which can thus be taken as an upper limit to the value of the reflectivity.

Two of the second-order effects (refraction of the incident beam towards the normal as it transverses the refractive index gradient, and attenuation of the beam in the shock 'front') can be easily allowed for, but the third effect—that of multiple reflections occurring in the (finite thickness) shock front—presents a problem of severe mathematical complexity. For the case of grazing incidence, Pert and Smy (1970) have obtained the following relationship:

$$R_2=\frac{(\theta'_1{}^{1/2}-\theta'_0{}^{1/2})}{\theta'_1{}^{1/2}} \tag{5}$$

where θ'_1 is the grazing angle of refraction ($=\frac{1}{2}\pi-\theta_1$). In the derivation of equation (5) the effect of multiple reflections reinforcing the final reflected beam is taken to be negligible, and R_2 thus represents a lower limit to the true reflectivity R:

$$R_2<R<R_1. \tag{6}$$

A series expansion of equation (5) gives

$$R_2=\frac{1}{4\theta'_0{}^4}\left(\frac{\delta n}{n}\right)^2\left\{1-\frac{5}{2}\frac{1}{\theta'_0{}^2}\left(\frac{\delta n}{n}\right)+\ldots\right\}. \tag{7}$$

For large angles θ'_0 or small values of δn (as found in most experimental situations) equations (4) and (7) both reduce to

$$R=\frac{1}{4\theta'_0{}^4}\left(\frac{\delta n}{n}\right)^2 \tag{8}$$

although the exact formula (equation (3)) must still be used at angles very close to grazing incidence ($\theta_0\geqslant 86°$, typically). The theoretical variation of R with angle as given by equations (3), (4), (5) and (8) is shown in figure 1 for a Mach 1·90 shock moving into air at 1 atmosphere, and the variation of R_1 with Mach number is shown in figure 2 for various angles θ'_0.

2.2. *Reflection from a curved surface*

For a curved reflector (shock front) of radius r_s moving in a shock tube of radius r_t, it is apparent that the grazing angle of incidence θ'_0 is no longer constant as the shock front traverses the interaction region with the light beam, but varies from $\theta'_0+\delta\theta$ to $\theta'_0-\delta\theta$, for a surface which is convex towards the downstream (lower refractive index) side, where

$$\sin\delta\theta\simeq\delta\theta=\frac{r_t}{r_s}. \tag{9}$$

We can then use equation (8) (except at extreme grazing incidence) to obtain the maximum and minimum reflected intensities I_1 and I_2 as the curved shock front traverses the interaction region:

$$I_1=\frac{1}{4}\left(\frac{\delta n}{n}\right)^2\frac{1}{(\theta'_0-r_t/r_s)^4} \tag{10}$$

$$I_2=\frac{1}{4}\left(\frac{\delta n}{n}\right)^2\frac{1}{(\theta'_0+r_t/r_s)^4} \tag{11}$$

so the shock front radius r_s is given by

$$r_s = \frac{r_t}{\theta'_0}\left(\frac{1+(I_1/I_2)^{1/4}}{1-(I_1/I_2)^{1/4}}\right). \tag{12}$$

This treatment is valid provided the radius of curvature r_s is sufficiently large that the diagnostic beam is reflected at essentially the same angle across its width d; that is, if the angle Δ subtended at the centre of curvature of the shock by the interaction region between the beam and the shock front is small compared with $\delta\theta$.

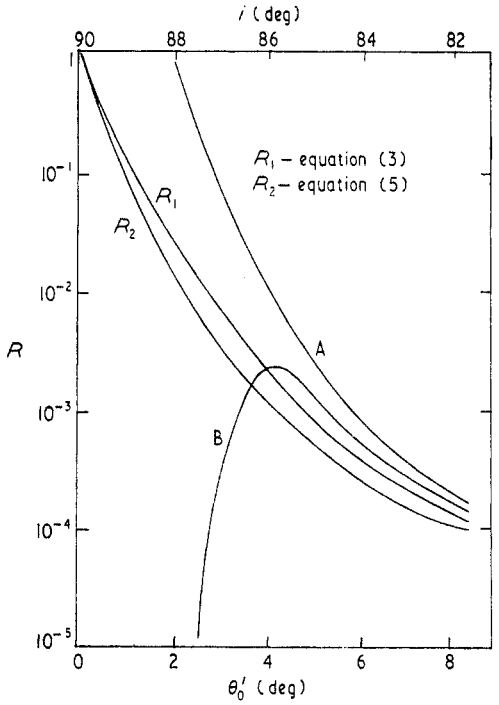

Figure 1. Reflection coefficient plotted against angle (theory) for a Mach 1·90 shock in air at 1 atmosphere. A, first-order theory (equation (8)); B, second-order theory (equation (4)).

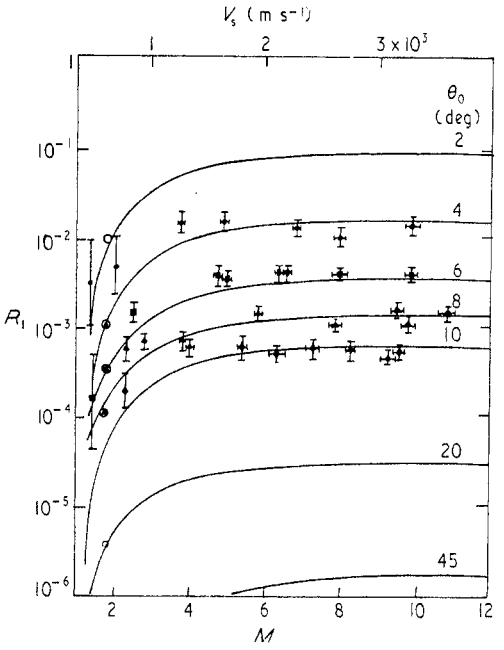

Figure 2. Reflection coefficient plotted against Mach number. ○, previous measurements at Mach 1·90 (Pert *et al.* 1970).

The angle Δ is given by

$$r_s\Delta = \frac{d}{\sin\theta'_0} \tag{13}$$

so, using equation (9) for $\delta\theta$, we require

$$\frac{d}{r_s\sin\theta'_0} \ll \frac{r_t}{r_s} \tag{14}$$

or

$$d \ll r_t \sin\theta'_0 \tag{15}$$

which is easily satisfied for any shock tube, even at very small values of θ'_0, by using a gas laser as the light source and focusing the beam to give very small values of d if necessary.

A more general treatment of the effects of perturbations of the shock front on a reflected light beam is given by Pert and Smy (1970) who obtain relationships which reduce to those given in equations (12) and (15) at angles near grazing incidence.

2.3. *Theory of curvature of shock fronts*

Hartunian (1961) and DeBoer (1963) have developed the theory of the curvature produced in a shock front by boundary-layer effects at the walls of a shock tube. The effect of the boundary layer is to distort the shock front to a parabolic profile, the vertex being situated at the shock tube wall. All the measurements to date on shock fronts in shock tubes have been too approximate to determine the exact profile of the shock front, so it is more useful to invoke the concept of the maximum protrusion X_m of the shock front from a plane surface through the point of contact of the shock front with the shock tube walls. For a spherical shock front of radius r_s, as assumed in §2.2, it is easily shown that

$$X_m = \frac{r_t^2}{2r_s} \tag{16}$$

for small values of X_m, so that X_m is a measure of the curvature $1/r_s$ of the (spherical) shock front.

DeBoer (1963) in an involved but still approximate analysis has determined the theoretical variation of X_m with Mach number for both laminar and turbulent boundary layers in a shock tube of circular cross section, the laminar boundary layer being appropriate to downstream pressures below 100 Torr, the turbulent boundary layer occurring at higher pressures. The theoretical curves of DeBoer (1963), recalculated for air as the downstream gas, are shown in figure 3. The curves intersect at Mach 3·5, which is the upper limit

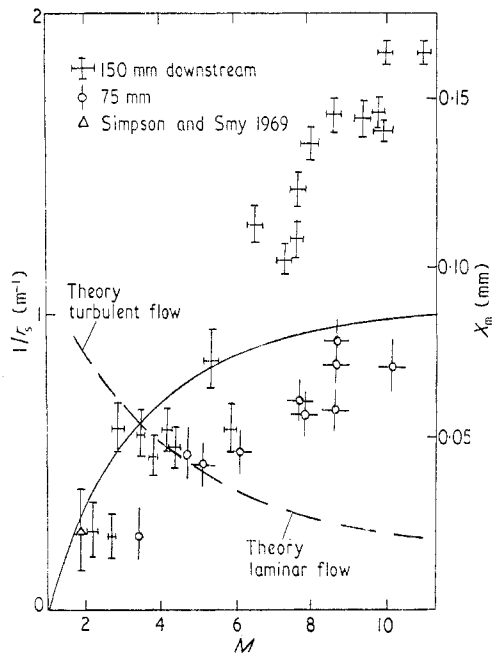

Figure 3. Shock curvature plotted against Mach number.

attained in previous experiments, so the majority of results (Duff and Young 1961, Linzer and Hornig 1963, Mazzella and DeBoer 1966) are too approximate to distinguish between the curves and are not shown. A single point from the results of Simpson and Smy (1969) is shown in figure 3 and this agrees well with the present results.

3. Experimental results

The shock tube used to produce shock waves having velocities of up to Mach 10, propagating into air at 1 atmosphere, has been described elsewhere (Davies and Simpson 1970). The beam from a 1 mW helium–neon laser is introduced through an aperture in the side of the shock tube, at grazing angles of 4–10°, and the beam reflected from the front of the shock wave as it approaches the aperture is detected by means of a photomultiplier (RCA type 8645) and displayed on an oscilloscope, simultaneously with a velocity measurement trace derived from two pressure probes (Atlantic Research Co., type LD25 blast transducers) or ionization probes mounted in the shock tube wall at a known distance apart. A 623·8 nm notch filter with a 2 nm passband was used to partially exclude the light from the ionized gas produced at the higher Mach numbers. The shock front reflectivity was calculated from the central portion of each reflected pulse, and the maximum to minimum reflected intensity ratio was used to calculate the shock front curvature $1/r_S$. The minimum intensity occurred at the start of each reflected pulse and the maximum intensity at the end, as expected from the geometry of the (convex downstream) shock front and optical system. The range of angles used was restricted at the lower end to 2° by the requirements of equation (15) (laser beam stopped down to 0·1 mm, shock tube radius 7·5 mm) and at the upper end to 10° by the rapid decrease of reflected intensity ($\propto 1/\theta'_0{}^4$) as the grazing angle is increased, to the point where the reflected signal cannot be distinguished above the background light from the shock-produced plasma, etc.

The measured reflection coefficients are plotted as a function of Mach number in figure 2 for the range of angles covered by the experiment. Also shown are some measurements from the earlier work of Pert *et al.* (1970) at a Mach number of 1·9, in a 25 mm radius pressure-driven shock tube. It will be seen that the measurements are in good agreement with theory (R_1) over the full range of experimental variables, and are also in agreement with the results of previous workers.

The shock front curvature measurements are shown as a function of Mach number in figure 3. The measurements were performed simultaneously with the reflectivity measurements and therefore cover a range of angles of incidence. No variation of measured curvature with angle was found. Most of the measurements were made at a point 150 mm downstream of the shock tube diaphragm (10 tube diameters), and some further measurements were made at a point 75 mm downstream of the diaphragm. It is apparent from figure 3 that the latter measurements confirm the existence of turbulent flow in the boundary layer at the wall of the shock tube, as expected, but the 150 mm measurements indicate that the boundary-layer thickness, and hence the shock front curvature, is still increasing (beyond the expected equilibrium value) as the shock wave propagates down the shock tube.

4. Discussion

4.1. *Shock front reflectivity*

Figure 2 shows that the reflectivity of a shock front can be reliably predicted at velocities up to Mach 10 and angles of incidence greater than 80°. In view of the very slow increase of reflection coefficient with Mach number at hypersonic velocities, it would seem reasonable to assume that the theory is still reliable at shock speeds of Mach 20–30. The consistency of the results and the agreement with previous measurements at low Mach numbers indicates that the angular variation of reflectivity can probably be predicted, using the theory outlined above, for angles of incidence in the range 45–60°. A reflection coefficient of about 10^{-6} would be expected for 45° incidence on a shock wave moving at Mach 20–30 into air at atmospheric pressure. This calls into question the validity of a number of recent measurements (Fünfer *et al.* 1963, Davies and Ramsden 1964, Ramsden and Davies 1964) of laser 'scattering' by rapidly moving or rapidly expanding plasmas, which are inevitably preceded by a shock wave. 'Scattering' coefficients of about 10^{-9} have been reported, and it is suggested that these figures may well merely represent the inefficient detection of the diagnostic light reflected from a highly curved shock front.

4.2. *Shock front curvature*

The results for shock front curvature are of a much more tentative nature than those for reflectivity. It is clear, however, that the existence of a turbulent boundary layer has been confirmed, and the boundary layer appears to develop steadily beyond the expected equilibrium value as the shock wave propagates down the shock tube. It is possible that the high values of curvature observed 150 mm downstream are caused by the proximity of the rarefaction wave which follows the shock wave down a shock tube (Wright 1961), gradually overtaking the shock wave and progressively perturbing the boundary layer, thus affecting the curvature. However, between the shock and rarefaction wavefronts a 'contact surface' separates the driver and driven gases, thus forming a second refractive index discontinuity following the shock front down the tube and which can be observed in these experiments at some angles of incidence to give a second reflected pulse. It is found that the contact surface is always 20 mm or more behind the shock, and the rarefaction wave is further still behind the shock front at the measuring section and is thus unlikely to have a large perturbing effect on the shock front at this distance (150 mm) downstream. The rarefaction wave finally overtakes the shock front some 200 mm down the tube, so any investigation of the further increase of curvature with propagation distance is precluded with the present shock tube. It is perhaps worth noting that there is no measurable decrease of Mach number down the shock tube, so the energy losses in the boundary layer can be assumed to be negligible.

5. Conclusions

It has been shown that appreciable reflection of a light beam by a hypersonic shock wave can be expected for shock fronts having radii of curvature of as much as 500 mm. The results are in good agreement with theory which can be extrapolated with a fair degree of reliability to the region where a number of experimenters have used optical diagnostic techniques on moving or expanding plasmas. For a laser-produced spark it seems probable that optical reflection from the shock front preceding the plasma will mask any scattering of the diagnostic light beam by the plasma.

Acknowledgments

This work was supported by the National Research Council of Canada, under grant No. A3666, and by the University of Alberta.

References

Born, M., and Wolf, E., 1970, *Principles of Optics*, 4th edn (Oxford: Pergamon Press), pp. 38–40.
Cowan, G. R., and Hornig, D. F., 1950, *J. chem. Phys.*, **18**, 1008–18.
Davies, C., and Simpson, D., 1970, *J. Phys.* E: *Sci. Instrum.*, **3**, 1000–2.
Davies, W. E. R., and Ramsden, S. A., 1964, *Phys. Lett.*, **8**, 179–80.
DeBoer, P. C. T., 1963, *Phys. Fluids*, **6**, 962–71.
Duff, R. E., and Young, J. L., 1961, *Phys. Fluids*, **4**, 812–20.
Fünfner, E., Kronast, B., and Kunze, H. J., 1963, *Phys. Lett.*, **5**, 125–7.
Greene, E. F., Cowan, G. R., and Hornig, D. F., 1951, *J. chem. Phys.*, **19**, 427–34.
Greene, E. F., and Hornig, D. F., 1953, *J. chem. Phys.*, **21**, 617–24.
Hartunian, R. A., 1961, *Phys. Fluids*, **4**, 1059–63.
Linzer, M., and Hornig, D. F., 1963, *Phys. Fluids*, **6**, 1661–8.
Mazzella, A. T., and DeBoer, P. C. T., 1966, *Phys. Fluids*, **9**, 892–5.
Pert, G. J., Seeds, G. M., Simpson, D., and Smy, P. R., 1970, *J. appl. Phys.*, **41**, 3516–20.
Pert, G. J., and Smy, P. R., 1970, *Can. J. Phys.*, **48**, 1521–7.
Ramsden, S. A., and Davies, W. E. R., 1964, *Phys. Rev. Lett.*, **13**, 227.
Simpson, D., and Smy, P. R., 1969, *J. appl. Phys.*, **40**, 4928–32.
Wright, J. K., 1961, *Shock Tubes* (London: Methuen).